Cell analysis solutions that help your research stand out
EMD Millipore is a division of Merck KGaA, Darmstadt, Germany
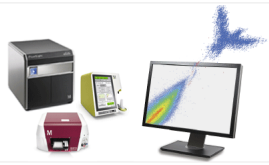
See for yourself

The Journal of Immunology

Myosin 1c Participates in B Cell Cytoskeleton Rearrangements, Is Recruited to the Immunologic Synapse, and Contributes to Antigen Presentation

José L. Maravillas-Montero, Peter G. Gillespie, Genaro Patiño-López, Stephen Shaw and Leopoldo Santos-Argumedo

J Immunol 2011; 187:3053-3063; Prepublished online 12 August 2011;
doi: 10.4049/jimmunol.1004018
http://www.jimmunol.org/content/187/6/3053

This information is current as of November 7, 2014.

Supplementary Material **http://www.jimmunol.org/content/suppl/2011/08/12/jimmunol.1004018.DC1.html**

References This article **cites 47 articles**, 30 of which you can access for free at:
http://www.jimmunol.org/content/187/6/3053.full#ref-list-1

Subscriptions Information about subscribing to *The Journal of Immunology* is online at:
http://jimmunol.org/subscriptions

Permissions Submit copyright permission requests at:
http://www.aai.org/ji/copyright.html

Email Alerts Receive free email-alerts when new articles cite this article. Sign up at:
http://jimmunol.org/cgi/alerts/etoc

The Journal of Immunology is published twice each month by
The American Association of Immunologists, Inc.,
9650 Rockville Pike, Bethesda, MD 20814-3994.
All rights reserved.
Print ISSN: 0022-1767 Online ISSN: 1550-6606.

Downloaded from http://www.jimmunol.org/ at Cinvestav del IPN on November 7, 2014

Myosin 1c Participates in B Cell Cytoskeleton Rearrangements, Is Recruited to the Immunologic Synapse, and Contributes to Antigen Presentation

José L. Maravillas-Montero,* Peter G. Gillespie,[†,‡] Genaro Patiño-López,[§] Stephen Shaw,[§] and Leopoldo Santos-Argumedo*

Myosin 1c (Myo1c) is a member of the unconventional class I myosins of vertebrates, which directly link the plasma membrane with the microfilament cortical web. Although this molecular motor has been implicated in cell functions such as cytoskeleton organization, cell motility, nuclear transcription, and endocytosis, its role in hematopoietic cells is largely unknown. In this study, we show that Myo1c is abundantly expressed in murine B lymphocytes and is preferentially located at the plasma membrane, especially in peripheral processes such as microvilli. We observed that this motor concentrates at the growing membrane protrusions generated during B cell spreading and that it is actively recruited to the immune synapse. Interestingly, Myo1c was detected in lipid rafts of B cells and showed strong colocalization with MHC-II, particularly after cross-linking of these molecules. By transfection of a dominant negative form of Myo1c or specific siRNA, we also detected alterations in the spreading and Ag-presenting ability of these cells. The data suggest that Myo1c is involved in the cytoskeleton dynamics and membrane protein anchoring or sorting in B lymphocytes. ***The Journal of Immunology*****, 2011, 187: 3053–3063.**

In recent years, cytoskeleton plasticity has been recognized as an important process in leukocytes. For example, by virtue of this plasticity, activated B lymphocytes are able to modulate their shape to extend their plasma membrane and cytoplasm in filopodia or lamellipodia (1). These extensions participate in cell spreading, which contributes to migration, activation, and Ag uptake (2). In lymphocytes, some of these events are controlled by cytoskeleton related proteins, including myosins (3–5), which are actin-dependent molecular motors. These proteins have an important role in motility of nonmuscle cells; for example, the nonmuscle myosin heavy chain IIA (MyH9/NMMHC-IIA) is associated with the uropod of crawling T cells (4).

There are more than 30 different classes of myosins. Class I myosins are formed by a unique heavy chain with an N-terminal motor or head domain, a central neck region, and a characteristic tail domain (TH1) that promote direct binding to phosphoinositides of the plasma membrane (6).

Vertebrate class I myosins consist of eight members (Myo1a-Myo1h) that have been implicated in nuclear transcription, lamellipodia generation in motile cells, brush-border dynamics of proximal-tubule cells of the kidney, adaptation of mechanoelectrical transduction in hair cells, as well as in exocytosis, adhesion, and vesicular trafficking in hematopoietic cells (6–11). One of the best studied roles of class I myosins is in stabilizing microvilli, most extensively analyzed in enteric epithelial cells where Myo1a mediates stabilization and protein sorting functions (12). These structures are formed by central actin filament bundles that are connected to the overlying plasma membrane by linking proteins, especially class I myosins.

The cytoskeleton has an important role in transmembrane protein localization, now recognized as a key element of immune responses such as the interaction of the TCR with MHC molecule–peptide complexes between a T cell and an APC, referred to as immunologic synapse (IS). For example, in studies of IS formation, when T cells are treated with actin-depolymerizing drugs, the TCRs fail to develop a polar distribution and cannot freely diffuse laterally (13). It has been suggested that an active actin-dependent process is responsible for moving or anchoring certain membrane proteins to defined locations (14, 15). Because myosins are the primary microfilament-associated motors, they represent likely candidates to mediate this function (16). In lymphocytes, myosin II has been reported to participate in IS formation, but not necessarily to contribute to polarization of signaling proteins to the synapse interface (4, 5).

We reported previously that mouse B cells express Myo1c (17) and that Myo1g is enriched at the membrane microvilli of human T lymphocytes (18). Given the potential role of class I myosins in regulating cytoskeletal and membrane reorganization, this study investigates the localization of Myo1c during B cell spreading and its possible role during IS formation. Our results confirm and extend the observation that Myo1c is abundantly expressed in B cells, particularly enriched in microvilli, and suggest a role for this molecule during IS formation and in Ag presentation.

Materials and Methods

Mice, cells, and reagents

Female C57BL/6J mice (6–8 wk of age) were used in all experiments except for the Ag presentation assays in which BALB/c mice of similar

*Departamento de Biomedicina Molecular, Centro de Investigación y de Estudios Avanzados del Instituto Politécnico Nacional, Mexico City CP 07360, México; [†]Oregon Hearing Research Center, Oregon Health and Science University, Portland, OR 97239; [‡]Vollum Institute, Oregon Health and Science University, Portland, OR 97239; and [§]Experimental Immunology Branch, National Cancer Institute, National Institutes of Health, Bethesda, MD 20892

Received for publication December 9, 2010. Accepted for publication July 7, 2011.

This work was supported by Consejo Nacional de Ciencia y Tecnología (Grant 56836). J.L.M.-M. is Fellow 203768 at Consejo Nacional de Ciencia y Tecnología.

Address correspondence and reprint requests to Dr. Leopoldo Santos-Argumedo, Departamento de Biomedicina Molecular, Centro de Investigación y de Estudios Avanzados del Instituto Politécnico Nacional Apartado Postal 14-740, CP 07360, D.F. México. E-mail address: lesantos@cinvestav.mx

The online version of this article contains supplemental material.

Abbreviations used in this article: DRM, detergent-resistant membrane; HEL, hen egg lysozyme; IS, immunologic synapse; KLH, keyhole limpet hemocyanin; MMV, membrane/microvilli fraction; MyH9/NMMHC-IIA, nonmuscle myosin heavy chain IIA; Myo, myosin; PI(4,5)P_2, phosphatidylinositol 4,5-bisphosphate; PNL, postnuclear lysate; SEB, *Staphylococcus* enterotoxin B; WB, Western blot.

www.jimmunol.org/cgi/doi/10.4049/jimmunol.1004018

Downloaded from http://www.jimmunol.org/ at Cinvestav del IPN on November 7, 2014

characteristics were used. The mice were produced at the Centro de Investigación y de Estudios Avanzados (Mexico City, Mexico) animal facility, and the animal care and use committee of Centro de Investigación y de Estudios Avanzados approved all experiments. Abs and reagents: R2652 (rabbit polyclonal IgG anti-Myo1c) and mT2 (mouse monoclonal IgG1 anti-Myo1c) (19), biotinylated NIM-R4 (monoclonal rat anti-MHC-II), biotinylated mouse anti-H-2K^d (BD Pharmingen), biotinylated rat IgG or mouse IgG (Jackson ImmunoResearch), goat anti-lamin B, goat anti-actin (both from Santa Cruz), mouse anti-β tubulin, Alexa488-labeled goat anti-rabbit IgG, HRP–anti-mouse IgG1 and HRP-anti-goat IgG, FITC-phalloidin, Pacific Blue anti-B220, PE anti-CD3 (BD Pharmingen), DAPI, phalloidin-rhodamine (Molecular Probes), streptavidin-Cy3, streptavidin-HRP, streptavidin-Sepharose beads (Zymed), protein G-Sepharose beads (Invitrogen), and biotinylated cholera toxin B subunit (Sigma). Mouse cell lines: Ag8, BCL-1, WEHI-231, 70Z/3, BaF/3, 3T3, BW5147 and RMA-S, IC21, and P815.

B lymphocyte isolation, activation, and immunofluorescence staining

Mononuclear cells were isolated from spleen by Ficoll-density gradient separation. B cells were enriched by panning, using plastic dishes coated with anti–Thy-1 mAb ascites (NIM-R1). For activation, 2×10^6 cells were incubated in 1 ml 10% FBS supplemented RPMI 1640 (Life Technologies) containing LPS from *Escherichia coli* O55:B5 at 50 μg/ml (Sigma) plus 10 U/ml IL-4 (Genzyme) for 48 h at 37˚C. For immunofluorescence staining, the cells were washed with PBS and fixed for 15 min with 4% paraformaldehyde, permeabilized with 0.1% of Triton X-100, and incubated with different Abs or fluorescent reagents as described previously (17).

RNA isolation and RT-PCR

RNA was obtained from 5×10^6 resting spleen B cells purified by magnetic based-negative selection (Miltenyi Biotec) using TRIZOL (Invitrogen). Purity of these isolated cells was no less than 95% determined by the expression of B220 by flow cytometry. The expression of the eight class I myosins was analyzed by a one-step RT-PCR system (Invitrogen) according to manufacturer's instructions. The primers used were reported previously (19); these were designed to amplify regions that span introns (to avoid amplification of genomic DNA) and were validated with control tissues.

Constructs, retroviral infections, and spreading assays

The chimeric sequence of N-terminal GFP linked to Myo1c (GFP-Myo1c) was cloned into a retroviral vector, pMSCVpuro (Clontech). Retroviral infections of 48-h activated primary B cells were performed by spin infection after collecting viral particles produced from the Plat-E packaging cells transiently expressing the retroviral construct. Transduced B cells were transferred to NIM-R8 (rat IgG2a anti-mouse CD44) precoated glass bottom Petri dishes and analyzed with an Olympus confocal microscope. All live imaging was done at 37˚C using a 63× objective. Other spreading assays mentioned in this study were performed with the same inducing anti-CD44 over glass cover slips; the cells were fixed, permeabilized, and stained with the different reagents enumerated previously. The preparations were analyzed with Leica or Olympus microscopes using 60× objectives and Olympus FluoView or NIH ImageJ software for measurements, correlation coefficient calculations, and spectral imaging. Other plasmids used were the pDEST732-based constructs: EGFP control, EGFP-tagged Myo1c TailIQ, and full-length Myo1c, described previously (20). These plasmids were transfected into A20 lymphoma by electroporation according to procedures established previously (21).

Detergent-resistant membrane isolation and immunoprecipitation assays

For lipid raft isolation, A20 cells (1×10^8) were washed with ice-cold PBS and lysed for 30 min on ice in 1% Triton X-100 in TNE buffer containing protease and phosphatase inhibitors (TNE: 10 mM Tris/HCl [pH 7.5], 150 mM NaCl, and 5 mM EDTA plus 2.5 mg/ml each of PMSF, leupeptin, aprotinin in DMSO, and 1 mM sodium orthovanadate). The mix was further homogenized with 10 strokes in a Wheaton loose-fitting dounce homogenizer. Nuclei and cellular debris were pelleted by centrifugation 10 min at $900 \times g$. For the discontinuous sucrose gradient, 1 ml of cleared supernatant was mixed with 1 ml of 85% sucrose in TNE and transferred to the bottom of a Beckman 14×95 mm centrifuge tube. The diluted lysate was overlaid with 6 ml 35% sucrose in TNE and finally 3.5 ml 5% sucrose in TNE. The samples were centrifuged 20 h at $200{,}000 \times g$ and 4˚C. Fractions of 1 ml were collected from the top of the gradient and then analyzed by dot blot or Western blot (WB) and subsequent densitometry using ImageJ software. A pool of rafts, consisting of Lyn-present buoyant fractions, were immunoprecipitated using biotinylated anti-MHC-II Ab NIM-R4 or rat IgG as isotype control. The reactions were incubated for 4 h, and then Ag–Ab complexes were precipitated using streptavidin-Sepharose (Zymed) maintaining the temperature at 4˚C during all procedures. Beads were washed with cold TNE and boiled in sample buffer. SDS-PAGE and WB analysis were performed according to standard protocols, searching for Myo1c using monoclonal mT2 Ab (19). The same procedures were used for MHC-I immunoprecipitation from rafts with mouse anti-H-2K^d, mouse IgG as isotype control, and protein G-Sepharose beads.

Microvilli isolation and protein content analysis

Panning-enriched spleen B cells (1×10^9) were resuspended in PBS containing 20% FBS and incubated for 20 min at 37˚C. Cells were passed through a $27^{1/2}$G needle five times to shear off the microvilli. The samples were centrifuged as described previously (13) for the isolation of membrane/microvilli fraction (MMV) and the postnuclear lysate (PNL) fraction. Both preparations were then analyzed by WB with conventional procedures.

MHC-II capping induction

Primary enriched B cells (1×10^6) were stained with biotinylated NIM-R4, incubating the sample 15 min at 4˚C. After that, the cells were washed with cold PBS and streptavidin-Cy3 was added incubating 10 min at 37˚C to induce cross-linking. Finally, the cells were fixed with 4% paraformaldehyde and permeabilized with 0.1% of Triton X-100 to detect Myo1c as is described below. After staining, the cells were mounted on cover slips treated with in poly-L-lysine (Sigma) for microscopy observations.

Conjugate formation and Myo1c detection

Conjugates were prepared as described (22) with some modifications. Forty-eight–hour activated B cells (1×10^6) were pulsed for 20 min with 5 μg/ml of *Staphylococcus* enterotoxin B (SEB; Toxin Technology) and mixed with panning enriched resting T cells (1:1) for 30 min. The cells were previously loaded with Cell Tracker orange (B cells) and blue (T cells) according to manufacturer's protocols (Invitrogen). For Myo1c staining, the cells were fixed with 3.7% paraformaldehyde, permeabilized with 0.1% Triton X-100 (Sigma) plus 5% goat serum, and incubated overnight at 4˚C with 0.3–1 μg anti Myo1c or nonspecific purified rabbit IgG (Cappel). Afterward, the cells were washed with PBS and incubated with 50 μl secondary fluorescent Abs diluted 1:200. Finally, cells were washed, adhered on poly-L-lysine-treated glass cover-slips (Sigma), and mounted with Vecta-Shield (Vector) for confocal microscopy or resuspended in 1% formaldehyde for flow cytometric analysis. To detect Myo1c accumulation in conjugates, we measured mean fluorescence intensity of both T/B interface zones and the rest of the B cell plasma membrane using ImageJ software. If the fluorescence intensity of Myo1c at the interface was at least 1.5-fold higher than at the rest of the cell membrane, the conjugate was considered Myo1c positive polarized. Both polarized and nonpolarized conjugates percentages in SEB+ or SEB− treated APCs were calculated.

Ag presentation assays

A20 transfectants, expressing the different Myo1c constructs, were sorted in a MoFlo cytometer (Dako Cytomation) by their expression of EGFP or EGFP-tagged proteins 48 h after electroporation. Cells were loaded with hen egg lysosome (HEL) at 10, 50, or 100 μg/ml or keyhole limpet hemocyanin (KLH) at 100 μg/ml, in RPMI 1640-supplemented media for 8 h. Subsequently, the medium was replaced and cells were mixed with splenocytes of BALB/c mice in a 1:8 ratio. These animals were previously immunized with 100 μg/ml HEL (Sigma) diluted in complete Freund adjuvant at day 0, again with same Ag concentration in incomplete Freund adjuvant at day 14, and finally with the same Ag dose 7 d before animal sacrifice. Cocultures were analyzed 24 h later with flow cytometry, staining cells with anti-B220 for B cell exclusion and anti-CD4 plus anti-CD69 to identify activated T cells. To determine the level of IL-2 secreted by activated T cells, supernatants of the same cocultures were analyzed by ELISA according to the manufacturer's procedures (R&D Systems).

Myosin 1c siRNA and Ag presentation assays with Myo1c knocked-down cells

A20 cells (1×10^7) were transfected with 1 nmol siGENOME SMART siRNA pool targeting mouse Myo1c (catalog no. M-040802-01; Dharmacon) by electroporation under conditions described previously (21). Nontargeting siGENOME SMART siRNA pool no. 2 was used as control (catalog no. D-001206-14-05; Dharmacon). The siRNA-mediated Myo1c knock-down was verified with WB analysis at 72 h after transfection and

Downloaded from http://www.jimmunol.org/ at Cinvestav del IPN on November 7, 2014

quantified by ImageJ or by flow cytometry staining cells with R2652 Myo1c polyclonal Ab. These cells were used 72 h after transfection for Ag presentation assays described previously.

Results

Class I myosin expression in mouse B lymphocytes

Despite multiple reported roles for class I myosins in many cell types, there is little information about these proteins in hematopoietic cells and even less in lymphocytes. Therefore, we searched for the presence of the eight members of this family in purified mouse spleen B cells by RT-PCR and WB. Using previously validated PCR screening primers for detection of these molecules (19), we found that B cells express three different class I myosin mRNAs: Myo1c, Myo1e, and Myo1g (Fig. 1*A*). To confirm these results, we checked protein expression in lysates from freshly isolated cells with WB (Fig. 1*B*). We found that these three different myosins were present in splenic B lymphocytes.

Myosin 1c is highly expressed in B lymphocytes but less abundant in T lymphocytes

One interesting feature about unconventional myosins is their differential expression pattern among different tissues, which could provide information about their particular functions in a specific cell type. Microarray analysis available from SymAtlas (http://biogps.gnf.org/) indicated that Myo1c is a broadly expressed short-tail class I myosin, but its expression in hematopoietic cells occurs preferentially in B cells and macrophages (23). Using WB analysis, we detected Myo1c in several mouse B cell lines (Ag8, BCL-1, A20, WEHI-231, 70Z/3, and BaF/3) and in other hematopoietic cell types such as macrophages (IC21), T cells (BW5147 and RMA-S), mast cells (P815), and 3T3 fibroblasts (Fig. 1*C*). Flow cytometric analysis confirmed the expression of Myo1c in primary mouse B lymphocytes. In contrast, T lymphocytes showed lower expression (Fig. 1*D*). We confirmed these observations with confocal microscopy (Fig. 1*E*).

Myosin 1c is localized at different membrane protrusions of B cells

Previous data from our group showed that Myo1c changes its location pattern in B cells during CD44-induced spreading (17). These observations were limited because of the inability of Ab staining to reveal the dynamic localization of Myo1c in living cells. For that purpose, we expressed the chimeric protein EGFP-Myo1c in primary B cells using a retroviral transducing system for mouse lymphocyte infection (24). We detected GFP-Myo1c in all membrane protrusions generated during the anti-CD44 induced B cell spreading. As shown in Fig. 2*A*, EGFP-Myo1c is localized in typical adhesion/motility-related protrusions such as lamellipodia and filopodia (white arrowheads), and is also visible at the longer highly dynamic dendrite-like protrusions (Fig. 2*B*), previously characterized in spreading experiments (25). It is important to highlight that images showed in Fig. 2*A* and 2*B* are focused in the optical plane nearest to the glass slides to visualize the thin membrane extensions. In other images, we showed midplane sections of cells where EGFP-Myo1c is localized in the plasma

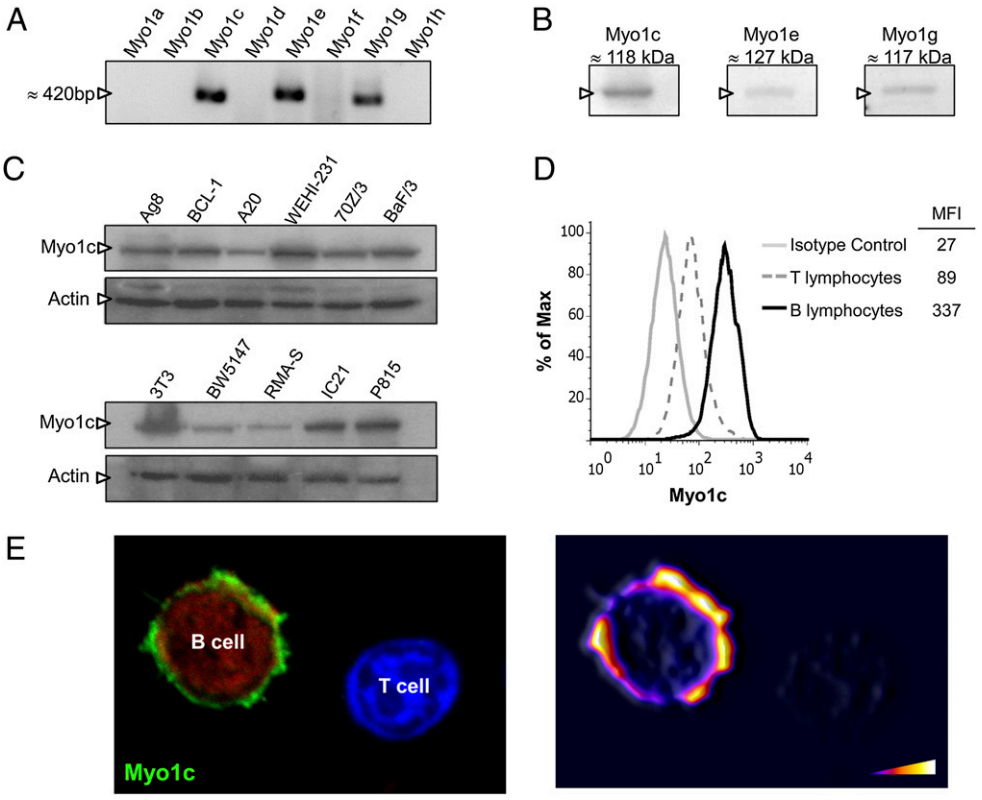

FIGURE 1. Class I myosin expression in lymphocytes. *A*, RT-PCR analysis of the eight class I myosin members in purified mouse splenic B lymphocytes. *B*, WB assays to confirm the expression of Myo1c, Myo1e, and Myo1g. *C*, WB for Myo1c in several mouse cell lines: Ag8 (plasmocytoma), BCL-1 (activated B cells), A20 (mature IgG$^+$ B cells), WEHI-231 (immature B cells), 70Z/3 (pre-B cells), BaF/3 (pro-B cells), 3T3 (fibroblasts), BW5147 and RMA-S (T cell lymphoma), IC21 (macrophages), and P815 (mastocytoma) along with the WB for actin as loading control. *D*, Expression levels of Myo1c measured by flow cytometry comparing B versus T lymphocytes; the mean fluorescence intensity (MFI) for each population is shown. *E*, In the *right panel*, purified primary splenic B and T cells were labeled in red (B cells) or blue (T cells) and stained for Myo1c. In the *left panel*, the high expression of Myo1c in B cells is easily detected compared with the low expression observed in T cells. The fluorescent signal of Myo1c staining, which is proportional to protein level, is shown as a spectral pattern according to the color scale given. Original magnification ~×1800.

Downloaded from http://www.jimmunol.org/ at Cinvestav del IPN on November 7, 2014

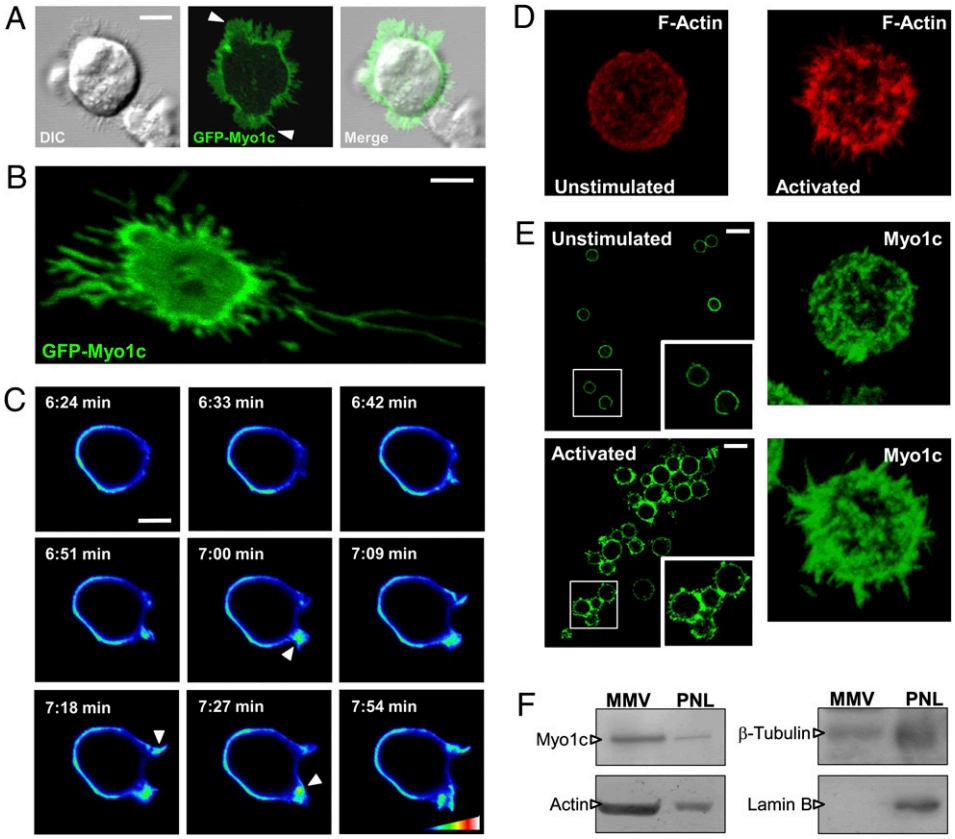

FIGURE 2. Myo1c is present and enriched in different membrane protrusions of B cells. *A* and *B*, Expression of GFP-Myo1c in filopodia or lamellipodia protrusions (*A*, white arrows) and dendrite-like extensions (*B*) formed during B cell spreading of primary mouse B cells. *C*, Enrichment of GFP-Myo1c at the membrane protrusions during B cell spreading. The color scale shows the relative fluorescence intensity, which is proportional to the concentration levels of myosin. Scale bars, 5 μm. *D*, B cell microvilli are inducible membrane structures, easily detectable by an F-actin staining with FITC-phalloidin after 48 h LPS plus IL-4 stimulation (compared with resting lymphocytes). *E*, Endogenous Myo1c is present in the membrane of unstimulated B cells and abundant at microvilli structures present in 48-h LPS plus IL-4–activated cells, the images show a single section (0.3 μm) and the maximal projection of one cell. Scale bars, 10 μm. *F*, Microvilli Myo1c enrichment in B lymphocytes assessed by the shear-based procedure described in *Materials and Methods*. Equal amounts (30 μg) of total protein of the MMV and the PNL were analyzed with WB for detection of Myo1c, actin (enriched in MMV fraction), β-tubulin, and lamin B (enriched at the PNL fraction).

membrane with enrichment at protruding areas and excluded from the nucleus (Fig. 2*C*, white arrowheads, and Supplemental Fig. 1*A*).

Interestingly, we also found Myo1c in B cell microvilli. Microvilli are plasma membrane protrusions present over the entire surface of resting lymphocytes (26) that differ in structure and function from lamellipodia–filopodia protrusions. It was previously demonstrated that microvilli are enhanced in number and length after stimulation of naive B cells (27); indeed, these structures may represent functional lymphocyte domains that allow molecule segregation. Analysis of human T cells and a mouse pre-B cell line demonstrated Myo1g enrichment in lymphocyte microvilli (18). We investigated whether Myo1c is also present at the same structures in B cells. We stimulated primary B cells with LPS plus IL-4 for 48 h to induce longer microvilli (Fig. 2*D*), which were then stained with anti-Myo1c Ab (R2652) and with fluorescent-labeled phalloidin for detection of F-actin. The cells were observed by confocal microscopy and compared with unstimulated B cells (Fig. 2*E*).

As shown in Fig. 2*E*, Myo1c was detected at the membrane in all cells. Its distribution was punctuate, rather than smooth, and was enriched in peripheral processes (microvilli), which are more visible in activated lymphocytes. To corroborate the microvilli enrichment of this protein, we used a previously reported mechanical shear-based procedure to isolate the MMV from cell bodies (PNL) (18). The data demonstrate that Myo1c is enriched in MMV compared with the PNL (Fig. 2*F*). Control proteins were assessed to validate the effectiveness of the fractionation; as expected, we confirmed the enrichment of actin, the absence of lamin B, and low levels of β-tubulin in the MMV fraction.

Extent of B cell spreading is dependent of Myo1c function

Expression of an EGFP-tagged Myo1-TH1 in cell lines causes a dominant negative phenotype (28, 29), which disrupts the targeting of endogenous class I myosins and confers cellular characteristics similar to those observed in Myo1a and Myo1e KO mice (12, 30). By transfecting an EGFP-tagged Myo1c–TH1 construct, we expected to block the function of endogenous Myo1c in the A20 mature mouse B cell line.

The constructs used in this study included a parental EGFP plasmid and two N-terminal EGFP tagged mouse Myo1c sequences, the first including the whole sequence of the protein (Myo1c full-length) and the other lacking the motor domain sequence, but includes the lipid-binding TH1 region and the calmodulin-binding IQ motifs (Myo1c IQ-Tail). When these constructs were expressed in A20 cells, they were detected by confocal microscopy according to its previously reported distribution (20), showed in Supplemental Fig. 1*B*. Soluble EGFP was homogeneously distributed in cytoplasm, but both EGFP Myo1c fusions were plasma membrane-associated as expected. WB analysis of

Downloaded from http://www.jimmunol.org/ at Cinvestav del IPN on November 7, 2014

the expressed fusion proteins confirmed their expected m.w. (Supplemental Fig. 1*C*).

Transient transfection, followed by selection by flow cytometry sorting, allowed us to compare spreading responses between A20 lymphocytes expressing the different constructs. We induced spreading over anti–CD44-coated glass coverslips, fixed and stained with phalloidine-rhodamine for F-actin detection. Therefore, we quantified spreading by determining the "shape factor" that resulted from the coefficient of length and width of a given cell. Values closer to 1.0 indicate a more rounded morphology; elongation of the cells then corresponds to factor values >1.0 and increases proportionally as the length of the cell increases.

We found that Myo1c IQ-Tail transfectants showed significantly lower shape factor values when compared with full-length Myo1c or control EGFP transfectants (Fig. 3*B*). This observation implies that lymphocytes expressing the dominant negative form of Myo1c cannot spread as much as the other groups of cells. These cells adopt a more rounded morphology compared with elongated, full-length Myo1c and EGFP constructs expressing lymphocytes (Fig. 3*A*).

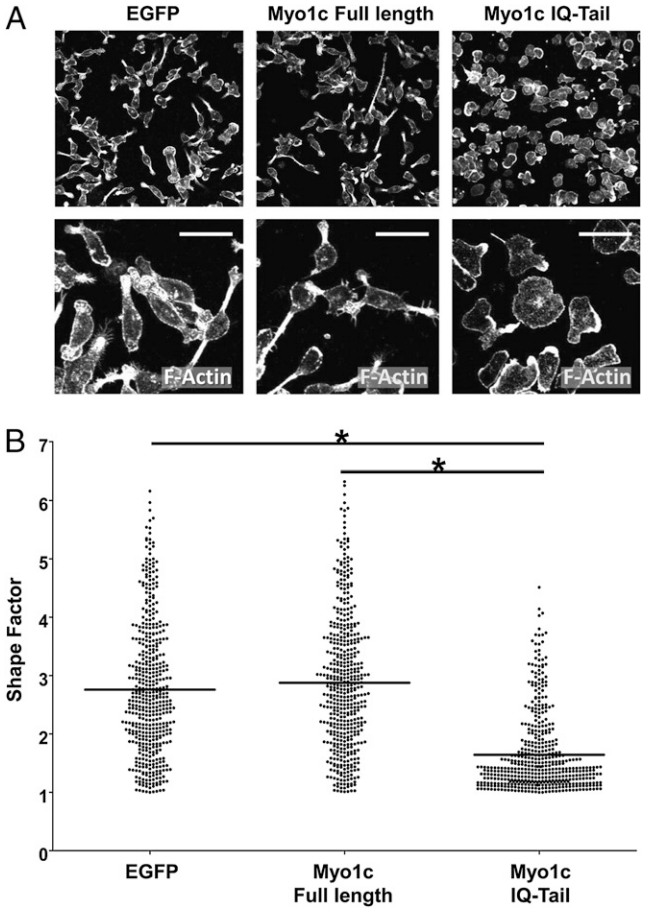

FIGURE 3. Spreading response in B cells is Myo1c dependant. *A*, A20 cells transfected with different constructs, Myo1c full-length, Myo1c tail-IQs, and EGFP were induced to spread over glass coverslips coated with anti-CD44 over 30 min. The cells were then fixed and stained to detect F-actin with rhodamine-phalloidin. Scale bars, 20 μm. *B*, The width and length of spread-transfected A20 cells were measured to determine "shape factor" values of each cell, which correspond to the coefficient of these two parameters. A total number of 12 fields for each condition were used to count 20 random cells per field. Each dot represents a single cell. Three different experiments were done; a representative one is shown. $*p < 0.05$ (two-tailed unpaired Student *t* test).

Lipid rafts of B lymphocytes contain Myo1c

Because Myo1c possesses a PH-like domain in the tail region, it is capable of direct interactions with the plasma membrane through binding to phosphoinositides such as phosphatidylinositol 4,5-bisphosphate [$PI(4,5)P_2$] (6). This lipid is present in the detergent-resistant membrane (DRM) domains, also called *lipid rafts* (31). It was previously reported that Myo1a, another member of class I myosins, associates with lipid rafts at the brush border of enterocytes. In addition, Myo1g was identified as a component of B cell DRMs (32).

We determined Myo1c association with DRMs by using two well-known approaches: immunolocalization of ganglioside GM1 with the B subunit of cholera toxin and detergent extraction followed by density gradient purification. When we stained primary

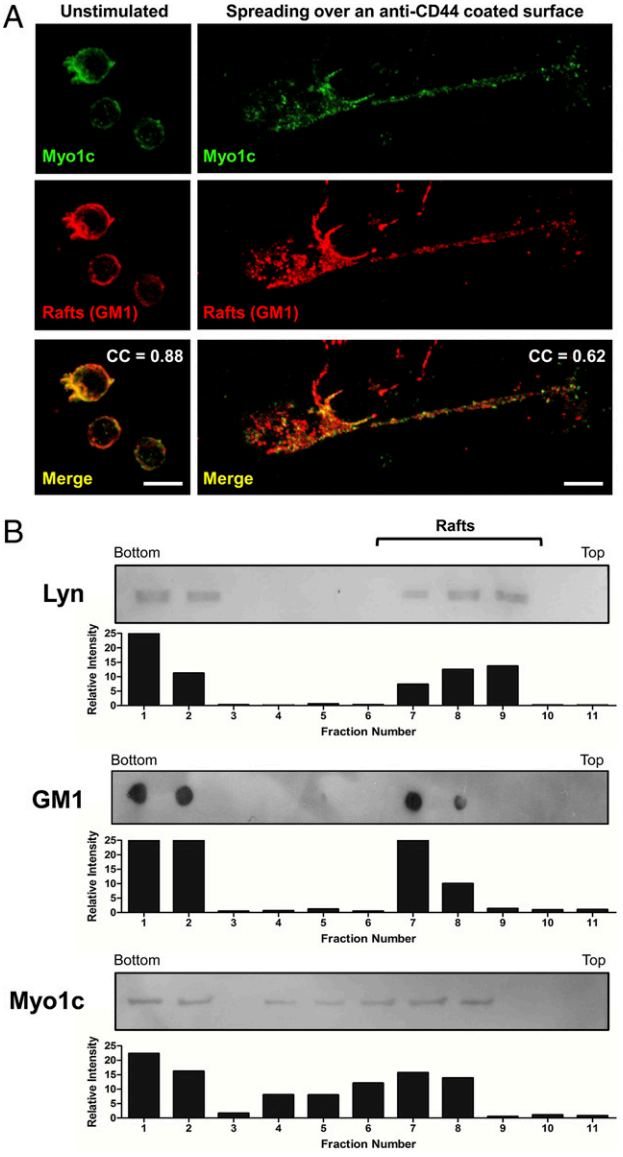

FIGURE 4. Lipid rafts of B cells contain Myo1c. *A*, Confocal projections of resting or CD44-stimulated primary spleen B cells that were stained for Myo1c and ganglioside GM1, a marker of lipid rafts. Scale bars, 10 μm. *B*, A20 cells were lysed using Triton X-100 at 4°C. The supernatant obtained was fractionated by sucrose density gradient to isolate buoyant DRMs. Equivalent volumes of all fractions (10 μl) were analyzed by dot-blot or WB to detect the presence and enrichment of Lyn and GM1, as raft markers, and Myo1c. Spots were analyzed by densitometry. Relative intensity of each blot is showed in corresponding graphs.

Downloaded from http://www.jimmunol.org/ at Cinvestav del IPN on November 7, 2014

splenic mouse B lymphocytes for detection of GM1, either rounded resting or activated cells, we distinguished zones of colocalization with Myo1c at the plasma membrane, as well as some spots of single fluorescent labeling (Fig. 4*A*). With raft isolation, we detected some of the Myo1c resident in DRMs, defined by the presence of the specific raft markers Lyn kinase and GM1. The rest of the Myo1c was clearly detected outside these membrane fractions (Fig. 4*B*).

MHC-II and Myo1c could be found in the same plasma membrane regions of B cells

It was previously demonstrated that Myo1a associates with lipid rafts in intestinal brush border microvilli, using fluorescence recovery after photobleaching. It was also shown that this protein participates in determining the localization and apical movement of some transmembrane proteins residing in these domains and promotes their movement to the plus-end of F-actin tracks forming the microvilli core (33). With a similar objective, we look for molecules that may be present at the same locations as Myo1c, in primary splenic mouse B cells.

Our analysis identified MHC-II molecules colocalizing with Myo1c. Interestingly, MHC-II molecules are present and enriched in B cell microvilli structures formed upon activation (Fig. 5*A*) (27). It is known that these actin-dependent structures can concentrate some transmembrane proteins but exclude others. As an example, B220 is mostly excluded from microvilli (34) and lipid rafts (35) in B cell lines.

To determine whether MHC-II and Myo1c are associated in lipid rafts, as suggested by confocal microscopy data, we performed an immunoprecipitation of these microdomains as described in *Materials and Methods*. When we used anti–MHC-II as capture Ab, we detected Myo1c in the WB (Fig. 5*B*). In contrast, when we immunoprecipitated rafts with anti–MHC-I, it was not possible to identify Myo1c in the samples (Fig. 5*B*, Supplemental Fig. 2*A*, *left panel*). As a control for MHC-I immunoprecipitation, we biotinylated cell surface proteins, extracted rafts, and immunoprecipitated MHC-I as described before, searching for its presence in the samples by using streptavidin-HRP (Supplemental Fig. 2*A*, *right panel*). In addition, colocalization of Myo1c with MHC-I was poor compared with the colocalization between Myo1c and MHC-II, defined by correlation coefficients showed in confocal sections of primary B cells in Supplemental Fig. 2*B* and 2*C*.

In addition to Myo1c being colocalized with MHC-II, we observed an interesting event when we induced capping by cross-linking MHC-II with Abs. As expected, MHC- II was accumulated at one pole of the lymphocytes, but a remarkable polarization of Myo1c was revealed (Fig. 5*C*). When the cells of these experiments were counted, we observed a mean of 62% of lymphocytes showing coclustering of Myo1c with MHC-II. The cells showing only MHC-II capping or no polarization of any molecule were less frequently observed (Supplemental Fig. 3). Note that not all the Myo1c signal was polarized to the point where class II molecules were present; there was some myosin staining in the rest of the cell membrane. Interestingly, in a more detailed observation we noticed that many cells showed a protruding structure at the pole where concentration of Myo1c and MHC-II were observed (Fig. 5*D*).

Myo1c localizes to the IS

Myosin IIA (i.e., MyH9/NMMHC-IIA) is the best characterized myosin in lymphocytes; it has an important role in motility and retrograde flow in T cells, but appears to be dispensable in establishing forward directed membrane movement of molecules during IS formation (4). Stimulated by these observations, we decided to look for a possible participation of Myo1c during the IS formation between B and T cells.

We assessed Myo1c distribution during SEB superantigen-induced IS formation between primary mouse T cells and B cell APCs. In the absence of SEB, Myo1c was distributed throughout the B cell membrane, including the contact site with T cells (Fig.

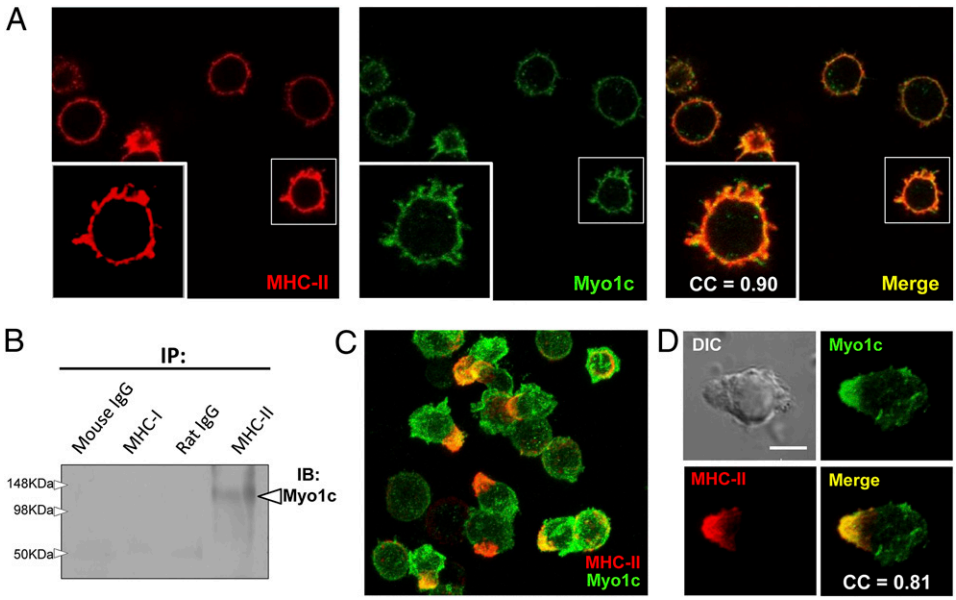

FIGURE 5. Myo1c and MHC-II are found in same B cell membrane locations. *A*, IL-4 plus LPS-activated spleen B cells were stained with anti–MHC-II and anti-Myo1c. It is possible to observe strong colocalization of both marks in the microvilli structures. Original magnification ~×800. *B*, A pool of DRMs isolated from A20 cells was immunoprecipitated with biotinylated mouse or rat IgG (as isotype controls) and biotinylated anti–MHC-I or anti–MHC-II, coupled to streptavidin-sepharose beads. The beads were collected and mixed with Laemmli buffer before analysis with WB using monoclonal anti-Myo1c. *C*, Activated primary B cells were incubated with biotinylated anti–MHC-II and streptavidin-Cy3 for 10 min at 37°C to induce capping. The cells were then fixed and stained with anti-Myo1c to detect colocalization between these proteins. Original magnification ~×500. *D*, It is possible to observe a prominent structure at the MHC-II capping pole of the cell colocalizing with an enriched stain of myosin 1c. Scale bar, 5 μm.

Downloaded from http://www.jimmunol.org/ at Cinvestav del IPN on November 7, 2014

6*A*). However, in the presence of SEB, the region of contact formed between the APC and T cell was enriched in Myo1c (Fig. 6*B*). We quantified the percentage of conjugates showing accumulation of Myo1c in the IS. In both control and toxin-treated cells, there was a significant increase of 35% when APCs were treated with SEB (Fig. 6*C*). Because the interface formed between B and T cells in a specific IS (SEB+) is flatter than the SEB− one, it is possible that surface proteins appear enriched there. To demonstrate that the polarization of Myo1c corresponds to a real enrichment of the motor protein, we localized IgM and B220 in SEB+ conjugates. Both molecules are transmembrane proteins highly expressed in B cells. Despite their abundance, there is no accumulation of these molecules at the IS interface as expected. In addition, as a positive IS control, staining for the TCR showed its enrichment at the contact region between both cells (Supplemental Fig. 4).

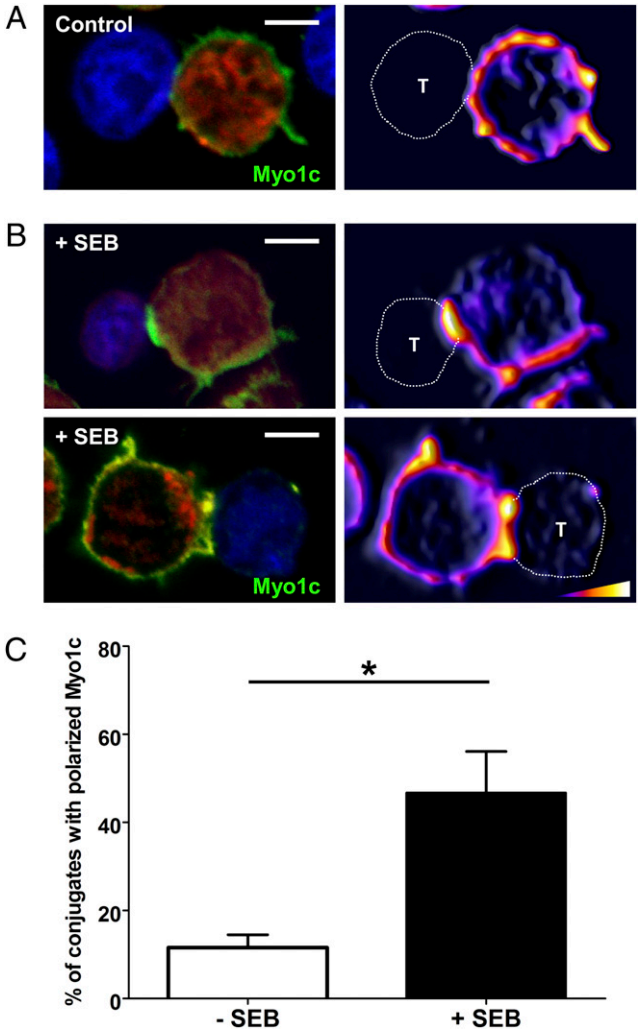

FIGURE 6. Myo1c is concentrated at the IS. Mouse primary B cells (fluorescent-red labeled) were mixed (1:1) with purified T cells (fluorescent-blue labeled) in the absence (*A*) or presence of SEB (*B*). An enrichment of the motor protein at the synapse is observed in two representative SEB-induced conjugates that are not present at the cell-cell contacts between non–toxin-treated lymphocytes. Images on the right depict the relative fluorescence intensity of Myo1c, using the color intensity scale in the bottom right. Scale bars, 5 μm. *C*, T cell–B cell conjugates were assessed for Myo1c polarization. A polarization coefficient was calculated for each conjugate by dividing the mean fluorescence intensity of Myo1c signal at the T cell-B cell interface by the mean fluorescence intensity of the rest of the APC membrane. When a conjugate gave a polarization coefficient >1.5, it was considered positively Myo1c polarized at the IS. The graph shows the percentages of positive Myo1c polarized T cell-B cell pairs, derived from the analysis of a total of 103 conjugates formed with SEB− or SEB+ treated B cells, in at least two independent experiments. *$p < 0.05$ (two-tailed unpaired Student *t* test).

Disruption of Myo1c affects the Ag-presenting function of B cells

On the basis set by the IS formation and MHC-II capping experiments described before, we decided to test whether Myo1c could be participating in Ag presentation processes. In our experiments, we used the different A20 transfectants previously described as APCs. These cells were loaded with different concentrations of HEL or control Ag KLH during 8 h before replacing of culture media. Loaded APCs were then mixed, with total splenocytes from previously immunized BALB/c mice with HEL Ag at 1:8 ratios of APCs to T cells. The cells were cocultured for 24 h and then analyzed by flow cytometry for CD69 upregulation on $CD4^+$ T cells. Supernatants of these cultures were also analyzed by ELISA to measure IL-2 secreted by those activated T cells.

The number of activated $CD4^+$ T cells was similar between the EGFP and the full-length Myo1c A20 transfectants. However, when we used A20 cells transfected with Myo1c Tail-IQ (dominant negative) as APCs, the number of activated $CD4^+$ T cells (Fig. 7*A*, 7*B*) and the amount of IL-2 secreted (Fig. 7*C*) was reduced at any of the three concentrations of HEL used in the assay. We also used APCs loaded with KLH as control Ag to detect the basal levels of CD4+CD69+ T cells.

As an alternative approach to evaluate the role of Myo1c in Ag presentation, we specifically knocked down Myo1c expression, and A20 cells were transfected with negative control or Myo1c-targeting siRNA pools. These cells were assayed for Myo1c expression by flow cytometry (Fig. 8*A*) and WB (Fig. 8*B*), finding a maximum decrease of protein level, near to 40% 72 h after transfection. When these siRNA-transfected A20 cells were used as APCs in the Ag presentation experiment described before, significant reductions in the percentage of $CD4^+CD69^+$ T cells (Fig. 8*C*) and IL-2 concentration (Fig. 8*D*) were observed comparing Myo1c-targeting siRNA with negative control siRNA transfected A20 cells.

Discussion

As shown in this study, Myo1c is one of the main class I myosins expressed in B cells. Previous observations from our group indicated that this molecule could be involved in cytoskeleton rearrangements of B lymphocytes, during the spreading induced by immobilized anti-CD44, B220, or MHC-II Abs (17). During live-cell observations using GFP tagged Myo1c, we observed strong localization of this molecule in all membrane protrusions generated during spreading in addition to enrichment of the protein at the points where membrane extensions begin to appear.

Class I myosins have been identified recently as key players in regulating cell deformation (28). Although overexpression of full-length Myo1c did not significantly alter the cell morphology; when endogenous myosin function is altered by using the dominant negative IQ–Tail construct, the spreading process is modified. The pictures show a nonpolarized spreading pattern, which means that the cells do not produce one or two long projections as control cells usually do. Instead, these lymphocytes generated broad surrounding lamellipodia that give them a flat, round shape. Myosin I-deficient *Dictyostelium* cells cannot properly control the generation of pseudopodia and directed cell migration (8). In hematopoietic cells, class I myosins are implied in the control of membrane forces: myosin 1f (Myo1f) KO mice present an exaggerated integrin-containing vesicles exocytosis in neutrophils, at-

Downloaded from http://www.jimmunol.org/ at Cinvestav del IPN on November 7, 2014

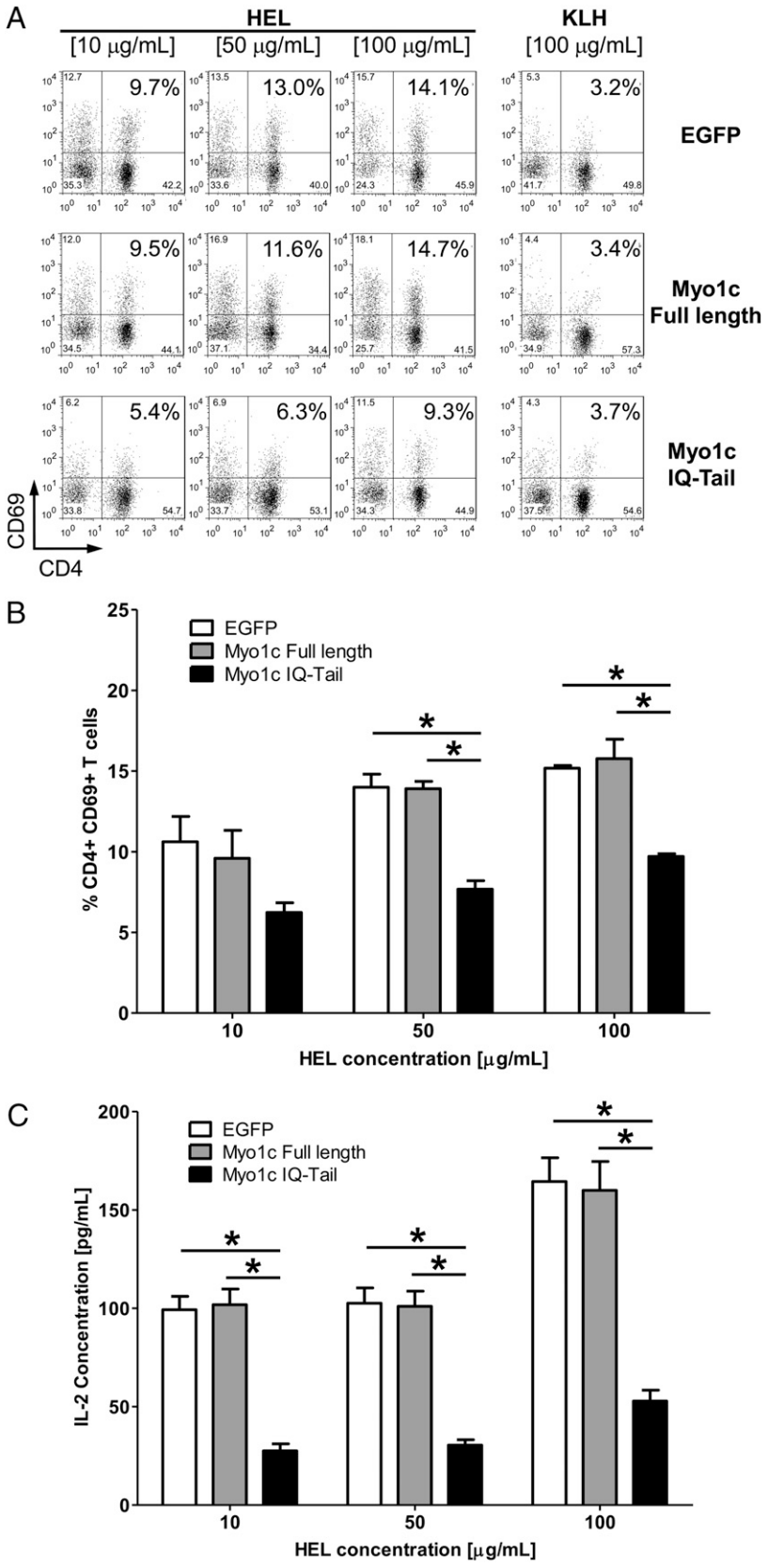

FIGURE 7. The disruption of Myo1c function decreases the Ag presentation ability of B cells. *A*, The A20 transfected cells described before were used as APCs by loading them with HEL or KLH at the concentrations shown. These cells were washed and mixed in a 1:8 ratio with total splenocytes obtained from BALB/C mice previously immunized with HEL. The cocultures were analyzed 24 h later with flow cytometry by measuring the expression of CD69 on CD4 T cell population. The dot plots indicate the percentage of $CD4^+CD69^+$ cells obtained for each experimental condition. *B*, The graph displays the data obtained from three independent experiments showing significant differences between the different APCs used. *C*, Supernatants of cocultures with different APCs were analyzed by ELISA to measure levels of IL-2 secreted by activated T cells. $*p < 0.05$ (two-tailed unpaired Student *t* test).

tributed to impaired connection between the cortical actin and the plasma membrane (36). The data obtained in this study suggest that Myo1c is one of the elements controlling the cytoskeleton–membrane interaction and cortical tension in B cells, and this protein could be participating in cell migration by generating or stabilizing the lamellipodia and filopodia observed during spreading. Our studies identify Myo1g and Myo1e as the other two class I myosins expressed in B cells. It remains to be seen whether their functions substantially overlap with those of Myo1c.

One interesting feature of Myo1c is its location in B cell microvilli. These structures were previously identified in the surface of activated B cells and have been suggested to be inducible

Downloaded from http://www.jimmunol.org/ at Cinvestav del IPN on November 7, 2014

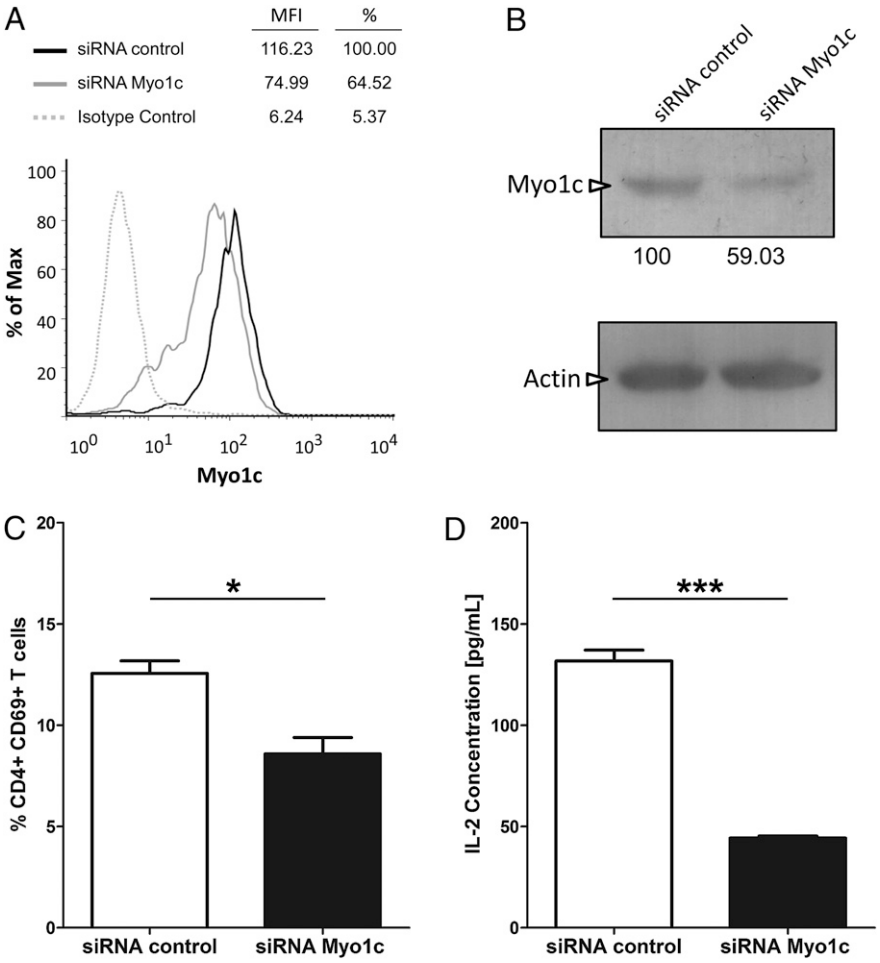

FIGURE 8. Specific knock-down of Myo1c decreases the Ag-presenting ability of B cells. *A*, A20 cells were transfected with either control siRNA or Myo1c siRNA. These cells were analyzed 72 h after transfection with flow cytometry to measure levels of endogenous Myo1c. The table shows the mean fluorescence intensity (MFI) of the histograms displayed, and the relative percentage of Myo1c reduction taking the MFI of control siRNA population as 100%. *B*, Both siRNA control and Myo1c-specific transfected A20 cells were lysed for protein extraction. The protein concentration of extracts was determined, and 50 μg of each one were resolved by SDS-PAGE and transferred to nitrocellulose to detect endogenous Myo1c. It is shown in the blot in the *upper panel* with relative densitometric quantification, taking the intensity given by control siRNA transfected cells as 100%. An actin load control is shown. *C* and *D*, Ag- presenting experiments described in Fig. 7 were performed using either control siRNA or Myo1c siRNA transfected A20 cells, loaded with 10 μg/ml of HEL and cocultured, as described before for 24 h, with spleen mononuclear cells of previously HEL-immunized BALB/c mice. Percentages of $CD4^+CD69^+$ recovered T cells (*C*) and secreted IL-2 concentrations measured by ELISA (*D*) are displayed in the graphs, which include data of four independent experiments. $*p < 0.05$, $***p < 0.0001$ (two-tailed unpaired Student *t* test).

domains that concentrate certain important molecules such as ICAM-1 or MHC-II (27). Microvilli likely are the initial contact sites for cell–cell interactions. Thus, Myo1c may segregate and anchor transmembrane signaling proteins to these microstructures in a manner similar to the function of Myo1a (another short-tail myosin) in enteric epithelial cells where it functions as a protein-segregating device. Myo1a, by its TH1 region, anchors lipid rafts that contain sucrase isomaltase. It has also been demonstrated that Myo1a interacts with these domains and probably directs their movement to the tip of the microvilli (12, 37). In this study, we have shown that Myo1c is enriched at B cell microvilli that lead us to speculate that this molecular motor may participate in the recruitment of receptors, adhesion molecules or signaling proteins to the microvilli. To support this speculation, we evaluated the association of Myo1c with B lymphocyte lipid rafts. By localizing GM1, it was possible to identify these membrane domains. Interestingly, when Myo1c was stained in the same cells, we observed partial colocalization spots. In previous descriptions of Myo1a, it was established that there are two different populations of this protein, defined by their association to rafts; one population has a high exchange rate between the cytoplasm and the membrane. The other, named *immobile*, is tightly associated with microvilli DRM domains (38). It is possible that the pattern observed for Myo1c in B cells is the result of similar regulation, showing the existence of one Myo1c population resident in rafts and other localized outside these domains. This assumption could also be supported by DRM isolation; although Myo1c can be separated in the raft fractions as expected, we also observed myosin in lower buoyant fractions, corresponding to nonraft associated protein.

According to previous data obtained with immunogold and TEM approaches (27), we detected an enrichment of MHC-II at microvilli in activated lymphocytes that show high colocalization with Myo1c, which implies the proximity between both proteins in those membrane protrusions. The most outstanding observation was related to the cocapping feature of Myo1c and MHC-II. When class II molecules were cross-linked at the B cell surface, it was possible to appreciate the aggregation of them at one cell pole. Interestingly, Myo1c is also polarized at the same location. It has been recognized that MHC-II molecules are immersed in DRMs, and their position allows them to initiate signaling events inducing maturation, proliferation, or cytokine production in B cells by recruitment and activation of Syk and Src family tyrosine kinases (39). The early events after MHC-II cross-linking in B cells, also includes calcium mobilization when using either monoclonal Abs or cognate T cells as ligands (40). It also has been observed in our spreading models that stimulation through MHC-II of activated B cells causes cytoskeleton rearrangements (1). Collectively, the data suggest a possible explanation of Myo1c and MHC-II polarization, because when cross-linking occurs, many activation signals induce cytoskeleton modifications, among other events. It was reported that MHC-II containing rafts accumulate at the ligation pole of the APC, concomitantly with actin polymerization at the same region (41). As calmodulin binding to Myo1c IQ domains is affected by Ca^{2+} concentration and modulates motor activity and binding to plasma membrane (42), the calcium mobilization induced in the activated B cell could affect myosin function. It is possible that motor molecules (attached to membrane and microvilli) become released of these locations to ac-

Downloaded from http://www.jimmunol.org/ at Cinvestav del IPN on November 7, 2014

cumulate at the actin polymerization region formed underneath the MHC-II cap. The motor activity, which can be activated by calcium or phosphorylation (43), may be related to anchoring or displacing MHC-II containing DRMs at the protruding structure formed at one pole of the B lymphocytes.

The idea that motor proteins could act as determinants of membrane topology and protein localization is not new. It has been suggested that an active actin-based process aids in moving proteins across the membrane (14–16). Based on this hypothesis, some groups have looked for the role of lymphocyte myosins such as MyH9/NMMHC-IIA in the reorganization of membrane receptors, like TCR, during IS formation. One study has reported that this motor protein regulates retrograde flow, but is dispensable for synapse assembly (4). Other authors found that this molecule is necessary for centripetal motion and fusion of signaling microclusters (5). However, they also reported that the concentration of actin, ezrin, and the TCR at the IS was not abolished after the inhibition of MyH9/NMMHC-IIA function. Thus, class I myosins emerge as possible candidates for active transport of membrane components to the IS interface. Noting the precedent of MHC-II polarization, we demonstrated Myo1c localization on the B cell side of the IS formed between T lymphocytes and activated B lymphocytes. Early interpretations of the IS proposed that the APCs passively participate during conjugate formation; however, this process requires a functional microfilament cytoskeleton for the polarization of lipid rafts containing molecules such as MHC-II (44). We anticipate that Myo1c is partially responsible for raft and protein mobilization given its enrichment at the synaptic interface. Myo1c, through its TH1 domain, binds directly to $PI(4,5)P_2$ (6), an abundant phosphoinositide in the cholesterol-rich rafts that contain MHC-II molecules in B cells (45). Because polarization of $PI(4,5)P_2$ at the T cell and APC sides of the IS has been reported recently (46, 47), we propose that Myo1c participates in this process. We hypothesize that it contributes to moving the rafts and their associated molecules across the membrane to the contact site at the B cell side.

If Myo1c has a role organizing the APC-T cell interface during IS formation, the disruption of its function would produce defects during Ag presentation processes. To confirm this idea, we performed experiments using the A20 cell line, transiently transfected with different Myo1c constructs. A20 transfectants overexpressing full-length Myo1c were used as APCs for HEL presentation to T cells. We observed similar yields of activated $CD4^+CD69^+$ T cells and secreted IL-2 when comparing these cells with control EGFP A20 transfected APCs. In contrast, Myo1c IQ-Tail A20 transfectants were significantly less efficient in inducing activated $CD4^+$ T lymphocytes or IL-2 secretion. In addition, when Myo1c was specifically downregulated in A20 cells by using siRNA, we also detected a decrease in $CD4^+CD69^+$ T lymphocytes or IL-2 secretion after the same Ag presentation assays. As the expression of the dominant negative form of Myo1c or the transfection with specific siRNA, reduces the ability of B cells as APCs, one possibility is that this motor protein contributes to regulation of Ag presentation by its localization at the immunologic synapse. An additional possibility is that Myo1c mediates these effects by regulating cell morphology and spreading. These findings establish that Myo1c has a previously unappreciated functional role in lymphocytes and should prompt further investigation of the precise mechanisms involved.

Acknowledgments

We thank Orestes López-Ortega and Héctor Romero-Ramírez for help at different stages of this work.

Disclosures

The authors have no financial conflicts of interest.

References

1. Santos-Argumedo, L., P. W. Kincade, S. Partida-Sánchez, and R. M. Parkhouse. 1997. CD44-stimulated dendrite formation ('spreading') in activated B cells. *Immunology* 90: 147–153.
2. Fleire, S. J., J. P. Goldman, Y. R. Carrasco, M. Weber, D. Bray, and F. D. Batista. 2006. B cell ligand discrimination through a spreading and contraction response. *Science* 312: 738–741.
3. Vascotto, F., D. Lankar, G. Faure-André, P. Vargas, J. Diaz, D. Le Roux, M. I. Yuseff, J. B. Sibarita, M. Boes, G. Raposo, et al. 2007. The actin-based motor protein myosin II regulates MHC class II trafficking and BCR-driven antigen presentation. *J. Cell Biol.* 176: 1007–1019.
4. Jacobelli, J., S. A. Chmura, D. B. Buxton, M. M. Davis, and M. F. Krummel. 2004. A single class II myosin modulates T cell motility and stopping, but not synapse formation. *Nat. Immunol.* 5: 531–538.
5. Ilani, T., G. Vasiliver-Shamis, S. Vardhana, A. Bretscher, and M. L. Dustin. 2009. T cell antigen receptor signaling and immunological synapse stability require myosin IIA. *Nat. Immunol.* 10: 531–539.
6. Hokanson, D. E., and E. M. Ostap. 2006. Myo1c binds tightly and specifically to phosphatidylinositol 4,5-bisphosphate and inositol 1,4,5-trisphosphate. *Proc. Natl. Acad. Sci. USA* 103: 3118–3123.
7. Krendel, M., and M. S. Mooseker. 2005. Myosins: tails (and heads) of functional diversity. *Physiology (Bethesda)* 20: 239–251.
8. Kim, S. V., and R. A. Flavell. 2008. Myosin I: from yeast to human. *Cell. Mol. Life Sci.* 65: 2128–2137.
9. Gillespie, P. G., J. P. Albanesi, M. Bahler, W. M. Bement, J. S. Berg, D. R. Burgess, B. Burnside, R. E. Cheney, D. P. Corey, E. Coudrier, et al. 2001. Myosin-I nomenclature. *J. Cell Biol.* 155: 703–704.
10. Foth, B. J., M. C. Goedecke, and D. Soldati. 2006. New insights into myosin evolution and classification. *Proc. Natl. Acad. Sci. USA* 103: 3681–3686.
11. Coluccio, L. M. 1997. Myosin I. *Am. J. Physiol.* 273: C347–C359.
12. Tyska, M. J., and M. S. Mooseker. 2004. A role for myosin-1A in the localization of a brush border disaccharidase. *J. Cell Biol.* 165: 395–405.
13. Krummel, M. F., M. D. Sjaastad, C. Wülfing, and M. M. Davis. 2000. Differential clustering of CD4 and CD3zeta during T cell recognition. *Science* 289: 1349–1352.
14. Braun, J., K. Fujiwara, T. D. Pollard, and E. R. Unanue. 1978. Two distinct mechanisms for redistribution of lymphocyte surface macromolecules. II. Contrasting effects of local anesthetics and a calcium ionophore. *J. Cell Biol.* 79: 419–426.
15. Braun, J., K. Fujiwara, T. D. Pollard, and E. R. Unanue. 1978. Two distinct mechanisms for redistribution of lymphocyte surface macromolecules. I. Relationship to cytoplasmic myosin. *J. Cell Biol.* 79: 409–418.
16. Tooley, A. J., J. Jacobelli, M. C. Moldovan, A. Douglas, and M. F. Krummel. 2005. T cell synapse assembly: proteins, motors and the underlying cell biology. *Semin. Immunol.* 17: 65–75.
17. Sumoza-Toledo, A., P. G. Gillespie, H. Romero-Ramirez, H. C. Ferreira-Ishikawa, R. E. Larson, and L. Santos-Argumedo. 2006. Differential localization of unconventional myosin I and nonmuscle myosin II during B cell spreading. *Exp. Cell Res.* 312: 3312–3322.
18. Hao, J. J., G. Wang, T. Pisitkun, G. Patino-Lopez, K. Nagashima, M. A. Knepper, R. F. Shen, and S. Shaw. 2008. Enrichment of distinct microfilament-associated and GTP-binding-proteins in membrane/microvilli fractions from lymphoid cells. *J. Proteome Res.* 7: 2911–2927.
19. Dumont, R. A., Y. D. Zhao, J. R. Holt, M. Bähler, and P. G. Gillespie. 2002. Myosin-I isozymes in neonatal rodent auditory and vestibular epithelia. *J. Assoc. Res. Otolaryngol.* 3: 375–389.
20. Patino-Lopez, G., L. Aravind, X. Dong, M. J. Kruhlak, E. M. Ostap, and S. Shaw. 2010. Myosin 1G is an abundant class I myosin in lymphocytes whose localization at the plasma membrane depends on its ancient divergent pleckstrin homology (PH) domain (Myo1PH). *J. Biol. Chem.* 285: 8675–8686.
21. Ying, H., J. F. Chang, and J. R. Parnes. 1998. PU.1/Spi-1 is essential for the B cell-specific activity of the mouse CD72 promoter. *J. Immunol.* 160: 2287–2296.
22. Patino-Lopez, G., X. Dong, K. Ben-Aissa, K. M. Bernot, T. Itoh, M. Fukuda, M. J. Kruhlak, L. E. Samelson, and S. Shaw. 2008. Rab35 and its GAP EPI64C in T cells regulate receptor recycling and immunological synapse formation. *J. Biol. Chem.* 283: 18323–18330.
23. Su, A. I., T. Wiltshire, S. Batalov, H. Lapp, K. A. Ching, D. Block, J. Zhang, R. Soden, M. Hayakawa, G. Kreiman, et al. 2004. A gene atlas of the mouse and human protein-encoding transcriptomes. *Proc. Natl. Acad. Sci. USA* 101: 6062–6067.
24. Tolar, P., H. W. Sohn, and S. K. Pierce. 2008. Viewing the antigen-induced initiation of B-cell activation in living cells. *Immunol. Rev.* 221: 64–76.
25. Sumoza-Toledo, A., and L. Santos-Argumedo. 2004. The spreading of B lymphocytes induced by CD44 cross-linking requires actin, tubulin, and vimentin rearrangements. *J. Leukoc. Biol.* 75: 233–239.
26. Brown, M. J., R. Nijhara, J. A. Hallam, M. Gignac, K. M. Yamada, S. L. Erlandsen, J. Delon, M. Kruhlak, and S. Shaw. 2003. Chemokine stimulation of human peripheral blood T lymphocytes induces rapid dephosphorylation of ERM proteins, which facilitates loss of microvilli and polarization. *Blood* 102: 3890–3899.

Downloaded from http://www.jimmunol.org/ at Cinvestav del IPN on November 7, 2014

27. Greicius, G., L. Westerberg, E. J. Davey, E. Buentke, A. Scheynius, J. Thyberg, and E. Severinson. 2004. Microvilli structures on B lymphocytes: inducible functional domains? *Int. Immunol.* 16: 353–364.
28. Nambiar, R., R. E. McConnell, and M. J. Tyska. 2009. Control of cell membrane tension by myosin-I. *Proc. Natl. Acad. Sci. USA* 106: 11972–11977.
29. Krendel, M., E. K. Osterweil, and M. S. Mooseker. 2007. Myosin 1E interacts with synaptojanin-1 and dynamin and is involved in endocytosis. *FEBS Lett.* 581: 644–650.
30. Krendel, M., S. V. Kim, T. Willinger, T. Wang, M. Kashgarian, R. A. Flavell, and M. S. Mooseker. 2009. Disruption of Myosin 1e promotes podocyte injury. *J. Am. Soc. Nephrol.* 20: 86–94.
31. Johnson, C. M., and W. Rodgers. 2008. Spatial Segregation of Phosphatidylinositol 4,5-Bisphosphate (PIP(2)) Signaling in Immune Cell Functions. *Immunol. Endocr. Metab. Agents Med. Chem.* 8: 349–357.
32. Saeki, K., Y. Miura, D. Aki, T. Kurosaki, and A. Yoshimura. 2003. The B cell-specific major raft protein, Raftlin, is necessary for the integrity of lipid raft and BCR signal transduction. *EMBO J.* 22: 3015–3026.
33. McConnell, R. E., and M. J. Tyska. 2007. Myosin-1a powers the sliding of apical membrane along microvillar actin bundles. *J. Cell Biol.* 177: 671–681.
34. Steegmaier, M., E. Borges, J. Berger, H. Schwarz, and D. Vestweber. 1997. The E-selectin-ligand ESL-1 is located in the Golgi as well as on microvilli on the cell surface. *J. Cell Sci.* 110: 687–694.
35. Cheng, P. C., M. L. Dykstra, R. N. Mitchell, and S. K. Pierce. 1999. A role for lipid rafts in B cell antigen receptor signaling and antigen targeting. *J. Exp. Med.* 190: 1549–1560.
36. Kim, S. V., W. Z. Mehal, X. Dong, V. Heinrich, M. Pypaert, I. Mellman, M. Dembo, M. S. Mooseker, D. Wu, and R. A. Flavell. 2006. Modulation of cell adhesion and motility in the immune system by Myo1f. *Science* 314: 136–139.
37. McConnell, R. E., J. N. Higginbotham, D. A. Shifrin, Jr., D. L. Tabb, R. J. Coffey, and M. J. Tyska. 2009. The enterocyte microvillus is a vesicle-generating organelle. *J. Cell Biol.* 185: 1285–1298.
38. Tyska, M. J., and M. S. Mooseker. 2002. MYO1A (brush border myosin I) dynamics in the brush border of LLC-PK1-CL4 cells. *Biophys. J.* 82: 1869–1883.
39. Al-Daccak, R., N. Mooney, and D. Charron. 2004. MHC class II signaling in antigen-presenting cells. *Curr. Opin. Immunol.* 16: 108–113.
40. Nashar, T. O., and J. R. Drake. 2006. Dynamics of MHC class II-activating signals in murine resting B cells. *J. Immunol.* 176: 827–838.
41. Delaguillaumie, A., V. Marin-Esteban, N. Setterblad, L. J. Leh, E. Assier, C. Gelin, D. Charron, A. Galy, and N. Mooney. 2008. Contrasting cytoskeletal regulation of MHC class II peptide presentation by human B cells or dendritic cells. *Eur. J. Immunol.* 38: 1096–1105.
42. Gillespie, P. G., and J. L. Cyr. 2004. Myosin-1c, the hair cell's adaptation motor. *Annu. Rev. Physiol.* 66: 521–545.
43. Yip, M. F., G. Ramm, M. Larance, K. L. Hoehn, M. C. Wagner, M. Guilhaus, and D. E. James. 2008. CaMKII-mediated phosphorylation of the myosin motor Myo1c is required for insulin-stimulated GLUT4 translocation in adipocytes. *Cell Metab.* 8: 384–398.
44. Setterblad, N., S. Bécart, D. Charron, and N. Mooney. 2004. B cell lipid rafts regulate both peptide-dependent and peptide-independent APC-T cell interaction. *J. Immunol.* 173: 1876–1886.
45. Knorr, R., C. Karacsonyi, and R. Lindner. 2009. Endocytosis of MHC molecules by distinct membrane rafts. *J. Cell Sci.* 122: 1584–1594.
46. Fooksman, D. R., S. R. Shaikh, S. Boyle, and M. Edidin. 2009. Cutting edge: phosphatidylinositol 4,5-bisphosphate concentration at the APC side of the immunological synapse is required for effector T cell function. *J. Immunol.* 182: 5179–5182.
47. Singleton, K. L., K. T. Roybal, Y. Sun, G. Fu, N. R. Gascoigne, N. S. van Oers, and C. Wülfing. 2009. Spatiotemporal patterning during T cell activation is highly diverse. *Sci. Signal.* 2: ra15.

Downloaded from http://www.jimmunol.org/ at Cinvestav del IPN on November 7, 2014